GSICS Global Space-based Inter-Calibration System

Quarterly

Newsletter Summer 2023 Issue

doi: 10.25923/bm5d-xb98
Vol. 17 No 2, 2023
Editor: Manik Bali, ESSIC UMD

CMA • CNES • ESA • EUMETSAT • IMD • ISRO • JAXA • JMA • KMA • NASA • NIST • NOAA • ROSCOSMOS . ROSHYDROMET • SITP • USGS • WMO

Articles

News in This Quarter

Announcements

GSICS Related Publications

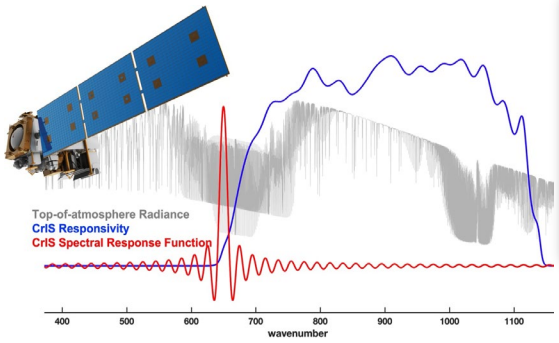

Figure 1. Conceptual diagram illustrating the CrIS idealized sinc SRF (spectrally stretched for clarity, red) with S-NPP long-wave responsivity (blue) for FOV5.

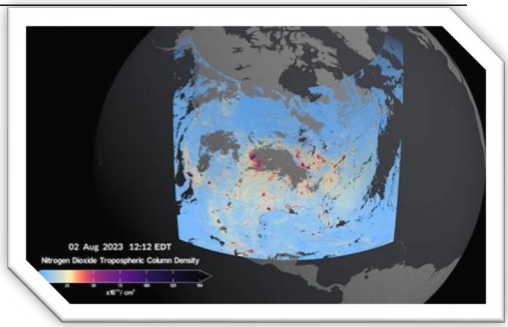

Image Above: First light image of TEMPO NO_2. Related article here. Courtesy of NASA SVS / SAO

Simulation of CrIS Radiances Accounting for Realistic Properties of the Instrument Responsivity That Result in Spectral Ringing Features

By Lori Borg [1], Michelle Loveless [1], Robert Knuteson [1], Hank Revercomb [1], Joe Taylor [1], Yong Chen [2], Flavio Iturbide-Sanchez [2] and David Tobin [1]. [1]CIMSS/SSEC UW-Madison, [2]NOAA NESDIS.

Recently, an article was published in **Remote Sensing** in 2023 [1] which provides a procedure for the simulation of radiances from the NOAA Cross-track Infrared Sounder (CrIS) Fourier Transform Spectrometer (FTS) to include spectral ringing effects caused by the finite-band, non-flat instrument spectral response to the incident radiation. A simulation using a line-by-line radiative transfer model is performed to illustrate the magnitude of the effect and to indicate which spectral channels are likely to be impacted.

Comparisons with CrIS observations are made to show that for most channels this effect is negligibly small compared to errors in the radiative transfer calculations, but for the longwave edge of the CrIS longwave band and a few other regions, the brightness temperature ringing is significant. While the ringing artifact described in this paper may appear to be removed when Hamming apodization is applied, as is done for the assimilation of CrIS data into Numerical Weather Prediction (NWP) models, it is still present, and its influence reappears if the spectral correlation induced by apodization is properly handled to preserve the information content that derives from high spectral resolution. Inclusion of the instrument responsivity in calculated spectra to properly mimic the observed spectra as defined in this paper eliminates artifacts from this type of ringing. Users of CrIS radiances should consider whether this effect is important for their application.

Characterization of CrIS Spectral Ringing Effects

Figure 1 provides an example of the CrIS responsivity for one of the CrIS S-NPP longwave detectors. Overlaid on the responsivity curve is a scaled sinc

doi: 10.25923/bm5d-xb98

spectral response function (SRF) that shows how an ideal FTS instrument weights nearby spectral points. The example SRF is artificially broadened in the wavenumber axis so that the extended side-lobes of the unapodized sinc function can be seen. For CrIS, the ideal SRF (i.e., with self apodization effects removed) is a sinc function with a zero-crossing consistent with the CrIS wavenumber grid spacing of 0.625 cm^{-1}. The sinc function shown is centered at the CrIS user grid band edge. Note that at the band edge at 650 cm^{-1} the responsivity has a strongly wavenumber dependent slope and the symmetrical SRF function has relatively large signal contributions from the high wavenumber side and relatively low signal contributions from the low wavenumber side. The process of radiometric calibration removes the broad-band shape of the CrIS responsivity. However, if unaccounted for, this asymmetry creates spectral artifacts that are often referred to as 'ringing', because they alternate between small positive and negative biases for every other optimally sampled point.

Methodology for Including Spectral Ringing in Calculated TOA Radiances

This paper presents the theory and methodology for calculating CrIS radiance spectra that include the spectral ringing behavior of the sensor and characterization of the nature and magnitude of the effects. This methodology includes the calculation of the CrIS responsivities and the computation of TOA radiances at high spectral resolution that include the ringing induced by the non-flat responsivity such that it is removed from the differences between observation and calculation. To characterize the effects of including the sensor response in the calculated radiance, comparisons are made to calculated radiances which do not incorporate the responsivity, but rather use one of two different artificial rolloffs to condition the monochromatic radiance calculations. The 'infinite-bandwidth' rolloffs represent the theoretical limit of no band-pass limitations, approximated by rolling off the calculations at a distance far away from the band edge. The 'band-edge' rolloffs, are used to represent what most general users or fast models use in their simulation of CrIS radiances and are defined to have the rolloffs go to zero at the same spectral location where the CrIS responsivities go to zero. These artificial rolloff functions are shown in the top panel of Figure 2.

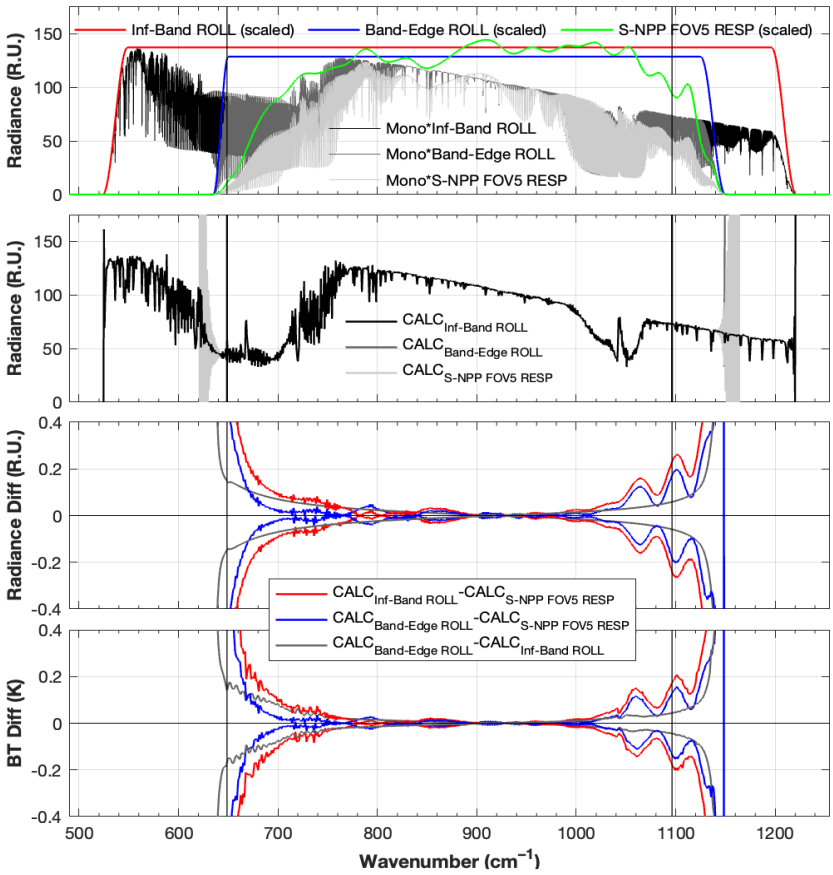

Figure 2. Calculated ringing effects for S-NPP LW band.

Figure 2 illustrates the impact of using responsivities versus rolloffs on calculations and the nature of S-NPP ringing for the LW band. This is done using an example calculated clear sky TOA spectrum. The top panel of this figure shows the calculated monochromatic spectra multiplied by the infinite-band rolloffs (black), the band-edge rolloffs (dark gray), and FOV5 responsivity (light gray). These are overlaid with the scaled rolloffs (red and blue) and responsivity (green). The second panel shows the CrIS Full Spectral Resolution (FSR) radiances for the cases with the infinite-band rolloffs, band-edge rolloffs, and FOV5 responsivity applied. The bottom two panels show the envelope of the ringing in radiance units (third panel from top) and in brightness temperature (bottom panel). The ringing is defined as the difference between the calculations with the rolloffs applied and the calculations with the FOV5 responsivity applied, with infinite-band rolloffs (red) and band-edge rolloffs (blue). This blue curve best characterizes the ringing in Obs-Calc differences made for band cut-offs employed by most users. Also shown is the difference between the

doi: 10.25923/bm5d-xb98

infinite-band rolloff result and the band-edge rolloff result (gray). The ringing effects are relatively small throughout most of the spectrum (< ±0.1 K), with the largest ringing effects at the longwave end of the longwave band reaching approximately ±0.5 K. The article also shows the ringing effects in the SW and MW bands for both S-NPP and NOAA-20 which have similar ringing characteristics across the bands.

Reference

[1] Borg, L., Loveless, M., Knuteson, R., Revercomb, H., Taylor, J., Chen, Y., Iturbide-Sanchez, F., and Tobin, D., 2023, Simulation of CrIS Radiances Accounting for Realistic Properties of the Instrument Responsivity That Result in Spectral Ringing Features. Remote Sens., 15(2):334. https://doi.org/10.3390/rs15020334.

Review of the Ground to Space CALibration Experiment (G-SCALE): Simultaneous Validation of UAV, Airborne, and Satellite Imagers for Earth Observation Using Specular Targets

By Brandon J. Russell[1], Raymond J. Soffer[2], Emmett J. Ientilucci[3], Michele A. Kuester[4], David N. Conran[3], Juan Pablo Arroyo-Mora[2], Tina Ochoa[4], Chris Durell[1] and Jeff Holt[11] Labsphere, Inc. [2] National Research Council of Canada [3] Rochester Institute of Technology [4] Maxar Technologies

Remote sensing is utilized by a wide range of scientific, government, and commercial entities for Earth Observation (EO). In the solar reflective wavelengths (~350 to 2500 nm), typical platforms include satellites, manned aircraft, and Unmanned Aerial Vehicles (UAVs). Each platform may host multiple sensor payloads, with advantages and disadvantages in spatial, radiometric, and temporal coverage and performance. Traditional ground-based vicarious calibration of EO assets relies on diffuse reflectance targets to relate sensor response directly to an absolute quantity, such as radiance ($W/m^2/nm/sr$) or surface reflectance.

While this method is effective, there are associated limitations in spatial scale and availability. The novel SPecular Array Radiometric Calibration (SPARC) method employs convex mirrors to relay the image of the solar disk to a sensor under test. With simultaneous solar radiometric measurements, SPARC is a SI traceable cal/val reference for either at-aperture radiance or surface reflectance [1]. The technique is inherently scalable over a wide range of spatial resolutions.

Figure 1. Primary target area. Mirror arrays are circled and labeled with the number of mirrors, with larger arrays for airborne and satellite (top right) and UAV (bottom left). Diffuse standards and spectral targets are visible.

The Ground to Space CALibration Experiment (G-SCALE) examined the intercalibration of multi- and hyperspectral sensors on satellite, aircraft, and UAV platforms in the VISNIR-SWIR wavelengths [2].

The experiment had three primary objectives: to perform simultaneous absolute radiometric calibration of three prominent EO platforms using both SPARC and diffuse methods, to directly compare data retrievals for both methods, and to generate a large data set for the development of inter-platform sensing technique.

doi: 10.25923/bm5d-xb98

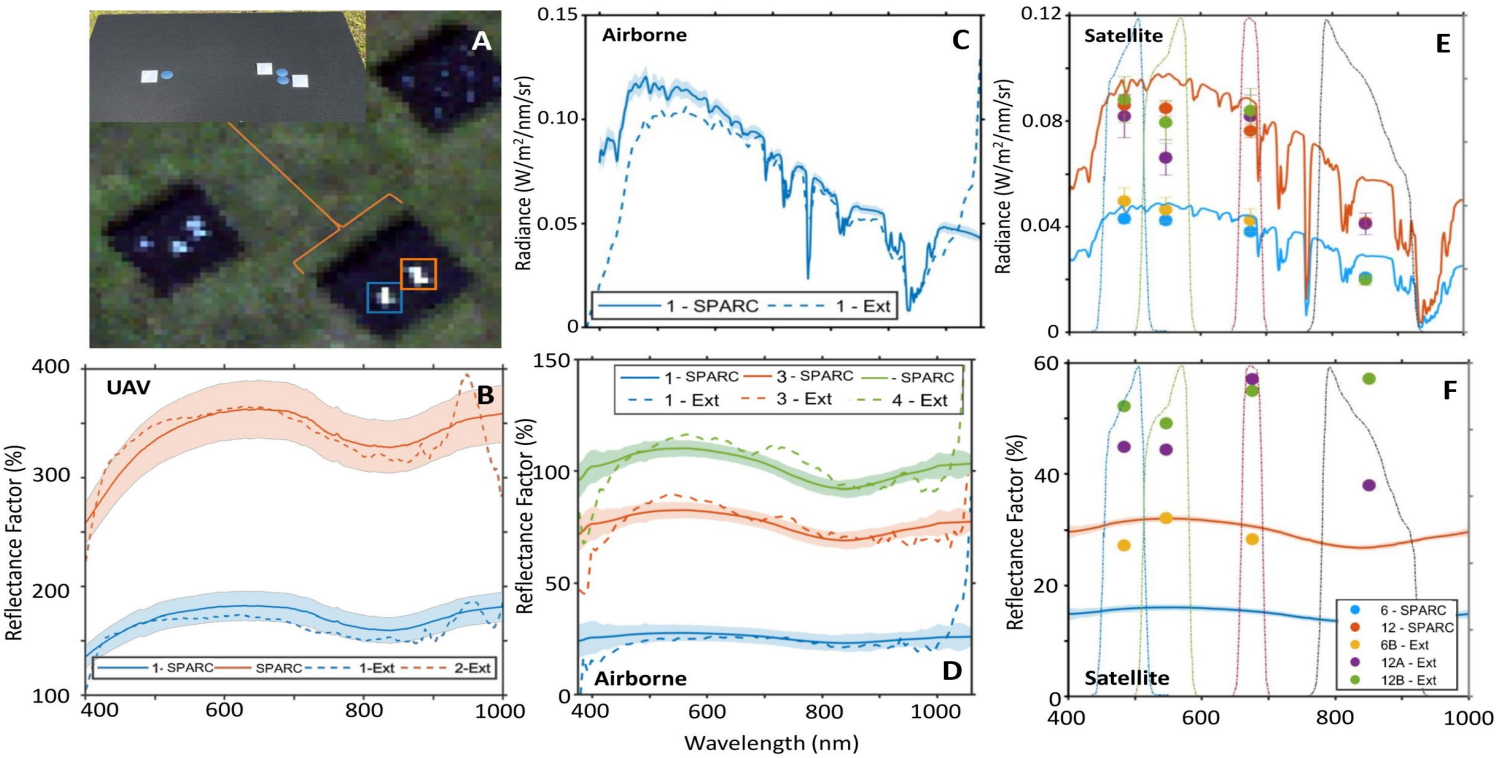

Figure 2. Mirror extractions (Ext) compared to predicted values (SPARC) from imagery in radiance (top row) and reflectance (bottom row). An example of mirror points observed in UAV imagery (top left).

The G-SCALE represents a unique, international collaboration between commercial, academic, and government entities. A brief summary of the experiment and VNIR results are presented here.

The experiment was carried out at the Rochester Institute of Technology's Tait Preserve in Penfield, NY, USA on 23 July 2021. Hyperspectral VIS-NIR and SWIR imagers mounted on UAV (Rochester Institute of Technology) and aircraft (National Research Council Canada) were flown over the target area, simultaneously with tasked observation by GeoEye-1 and Worldview-2 multispectral satellites (Maxar). Diffuse reflectance and SPARC mirror standards (Labsphere, Inc.) were deployed, alongside a variety of validation targets and instrumentation (Figure 1). In-situ solar irradiance data were continuously logged, and hyperspectral reflectance for all major standards and targets in-scene was measured. Atmospheric conditions remained highly stable and cloud-free.

For airborne and satellite sensors, previous radiometric calibrations were applied to raw imagery. For the aircraft sensor, DN-to-radiance coefficients were applied to the raw image to produce at-aperture radiance imagery. For the satellites, Maxar provided top-of-atmosphere radiance data calibrated using traditional reflectance-based methods in 2018[2]. The radiance of selected SPARC targets was extracted from the imagery and compared with radiance predicted based on mirror configuration, solar irradiance, atmospheric transmission, and reference sensor[2]. For UAV and airborne sensors, imagery was converted to surface reflectance using in-scene diffuse standards, while satellite imagery was processed to surface reflectance using Maxar's proprietary Atmospheric Compensation (AComp) algorithm[3]. For each platform, the reflectance of test SPARC targets was retrieved and compared to that predicted by a transformation of the predicted radiance[2].

Across platforms, good agreement was seen between traditional calibration methods and SPARC targets (Figure. 2). For the UAV, while radiometrically calibrated imagery was not available, the reflectance[1] of extracted mirror points (Figure. 2A) matched predictions to within the estimated uncertainty (Figure. 2B). The uncertainty in retrieval is large (~7.2%, $k = 1$) due to relative motion of the non-gimbled sensor creating uncertainty in the sensor ground sampling distance, as well as potential issues with signal smear and oversampling due to the physical swinging of the push-broom imager over the targets[4]. The UAV results illustrate the potential impact of platform operation to radiometric accuracy of imagery. In aircraft imagery, extracted radiance matches

predicted radiance to within the uncertainty (~3.6%, k = 1) over most wavelengths (Figure. 2C). Low retrieval below 450 nm is likely due to detector sensitivity and non-linearity, while elevated signal above 1000 nm is believed to be the result of detector architecture and aircraft motion. This trend was also observed for retrieved mirror reflectance (Figure. 2D). While not all mirror targets were observable in the satellite imagery, a selected GeoEye-1 top-of-atmosphere radiance image showed general agreement to SPARC predicted radiance (Figure. 2E) for each band (blue, green, red, NIR) within measurement uncertainty (~3.6%, k = 1). By contrast, there is a strong absolute bias and spectral shape in retrieved surface reflectance of the SPARC targets in the imagery that had been processed from top-of-atmosphere radiance to atmospherically corrected surface reflectance, relative to predicted values (Figure. 2F). This bias is not evident in the reflectance of large homogeneous targets and is under investigation.

Data harmonization and interoperability between remote sensing platforms will be key to enabling the potential of future EO missions. Ensuring consistent data quality between products at different spatial, temporal, and spectral resolutions will require innovative methods and technologies. The SPARC method represents one such tool, particularly if utilized in an automated and accessible network[5]. Multiple studies utilizing the G-SCALE data set are in progress and follow on experiments have been carried out. Preliminary results using traditional diffuse reflectance calibration methods yielded good agreement with UAV and aircraft platforms, and first order agreement to satellite retrievals with bias that could be attributed to known and correctable factors.

References:

1. Schiller, S. J. & Silny, J. The Specular Array Radiometric Calibration (SPARC) method: a new approach for absolute vicarious calibration in the solar reflective spectrum. in (eds. Ardanuy, P. E. & Puschell, J. J.) 78130E (2010). doi:10.1117/12.864071.

2. Russell, B. J. *et al.* The Ground to Space CALibration Experiment (G-SCALE): Simultaneous Validation of UAV, Airborne, and Satellite Imagers for Earth Observation Using Specular Targets. *Remote Sens.* **15**, 294 (2023).

3. Pacifici, F. *Validation of the DigitalGlobe surface reflectance product*. 1975 (2016). doi:10.1109/IGARSS.2016.7729508.

4. Conran, D. N. & Ientilucci, E. J. A Vicarious Technique for Understanding and Diagnosing Hyperspectral Spatial Misregistration. *Sensors* **23**, 4333 (2023).

5. Russell, B. *et al.* Initial results of the FLARE vicarious calibration network. in *Earth Observing Systems XXV* (eds. Butler, J. J., Xiong, X. (Jack) & Gu, X.) 14 (SPIE, 2020). doi:10.1117/12.2566759.

Characterization of the East-West Spatial Uniformity for GOES-16/17 ABI Bands Using the Moon

By Fangfang Yu (UMD), Xiangqian Wu (NOAA), Xi Shao (UMD) and Haifeng Qian (GST)

The NOAA Geostationary Operational Environmental Satellite (GOES) Advanced Baseline Imager (ABI) features two scan mirrors that can independently and simultaneously scan in the north-south (NS) and east-west (EW) directions. To validate the uniform response across varying scan angles within ABI's Field of Regard (FOR), NOAA designed and executed a series of special scans using in-orbit measurements during the post-launch test and post-launch product test (PLT/PLPT) period. For the infrared bands, the uniform background of space is used to validate the scan mirror emissivity corrections across all the scan angles. However, validating in-orbit spatial uniformity for the visible and near-infrared (VNIR) bands (Table 1) presents a challenge, as there is no such stable uniform bright target within the FOR. This article outlines a method that utilizes the Moon, which frequently appears in the space in between the Earth and the instrument's FOR boundary, to characterize spatial uniformity in the EW direction for the GOES-16/17 ABI VNIR data [1].

NOAA first used the Moon to characterize the EW spatial uniformity for GOES-15 Imager visible band. This was achieved by employing a series of rapid scans of a bright Moon as the spacecraft was rolled northward to capture the Moon when it passed through the space above the Earth's North Pole [2].

doi: 10.25923/bm5d-xb98

Band Name	Central wavelength (μm)	Detector type	Nominal IFOV (μrad)		# Rows	SNR SPEC at 100% albedo
			EW	NS		
B01	0.47	Si	22.9	22.9	676	300:1
B02	0.64	Si	12.4	10.5	1460	300:1*
B03	0.87	Si	22.9	22.9	676	300:1
B04	1.38	MCT	51.5	42.0	372	300:1
B05	1.61	MCT	22.9	22.9	676	300:1
B06	2.25	MCT	51.5	42.0	372	300:1

Table 1. Characteristic of ABI VNIR bands. MCT=Mercury Cadmium Telluride, Si=Silicone, IFOV= Instantaneous Field of View, SNR SPEC = Signal-to-Noise Ratio Specification. All the GOES-16/17 ABI VNIR bands meet the SNR SPEC requirements.
* except < 1% smaller than 300 and greater than 150.

Unlike with GOES-15, no such special spacecraft maneuver is required for ABI. It can scan the Moon whenever it appears in the space within FOR surrounding the Earth (Figure 1), thereby covering the full scan ranges of the instrument.

During the PLT/PLPT period, several "lunar chasing" events were conducted to intensively collect lunar images with the MESO scans in the nominal timeline as the Moon traversed space from west to east. Each chasing event lasted approximately 10 to 60 minutes, depending on the Moon's location within the FOR. The EW Response Versus Scan-angle (RVS) was analyzed using normalized ratios between the measured and simulated lunar irradiance at varying scan angles. These analyses were based on data combined from the multiple chasing events for each satellite, as described by Equations 1 and 2. Each lunar image was screened and subset for lunar irradiance calculation. The Global Space-based Inter-Calibration System (GSICS) Implementation of the ROLO (GIRO) model was employed to simulate the lunar irradiance for each image [3].

$$Norm\_Ratio_{e,t} = \frac{\frac{I\_ABI_{e,t}}{I\_GIRO_{e,t}}}{\text{mean}(\frac{I\_ABI_{e,t}}{I\_GIRO_{e,t}})} \ldots.(1)$$

where $I\_ABI_{e,t}$ is the lunar irradiance measured by ABI at time t in the chasing event e; and $I\_GIRO_{e,t}$ is the lunar irradiance simulated by GIRO model for the corresponding lunar data acquisition time. For each ABI image, the lunar irradiance is calculated with Equation (2).

$$I_{ABI} = \frac{\Omega}{f_{oversampling}} \sum_i^{row} \sum_j^{col} R_{i,j} \ldots(2)$$

where $R_{i,j}$ is the radiance for the sample at row i and column j in the subset image; Ω and $f_{oversampling}$ are the sample solid angle and oversampling factor for a given band and they are considered as constant values for each sample in an ABI image; and *row* and *column* are the size of the subset image. *Column* is height of focal plane array, and *row* is slightly wider than *column*. The size of the subset image, with the Moon near the center of an image, is chosen to ensure the scattered light from the Moon are accounted for as part of the lunar irradiance. The initial RVS results for the six VNIR bands are shown in Figures 2 and 3 for GOES-16 and 17 ABI, respectively. Both

Figure 1. Illustration of ABI FOR (the circle in thin dotted line), with the Earth in the center and the Moon traversing part of ABI's FOR as an example (in red dashed line).

satellites exhibit the largest variation in the normalized ratios at B01 (>1%), followed by a smaller variation at B02, and then within 0.5% at the long-wavelength bands. Analyses of the calibration data and lunar images indicate that the variations at B01-B03 are primarily due to the impacts of straylight from the Earth on certain lunar images during the lunar chasing events, including (1) Earthshine scattered into the spacelook scenes near the polar regions, and (2) light from the illuminated Earth leaking into space near the Moon.

doi: 10.25923/bm5d-xb98

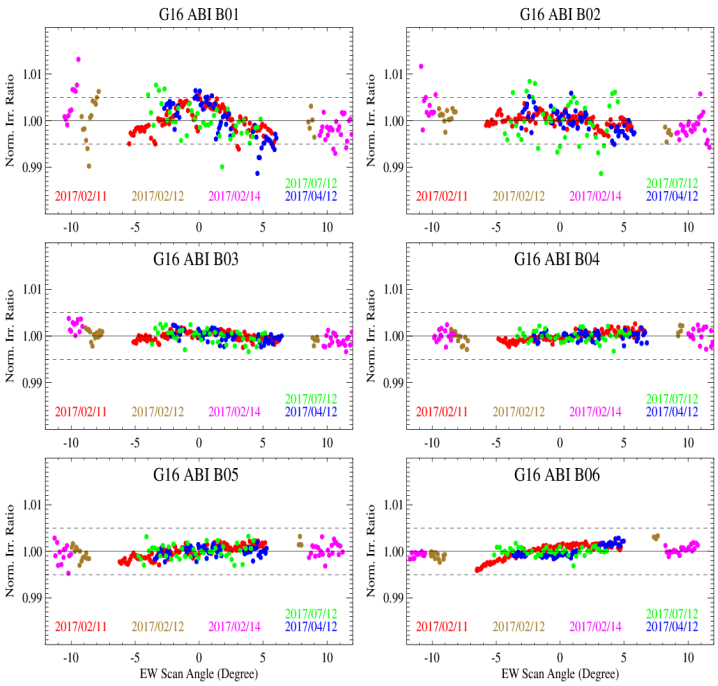

Figure 2. The normalized irradiance ratio values versus scan angles for G16 VNIR bands. The dashed gray lines are ±0.5%.

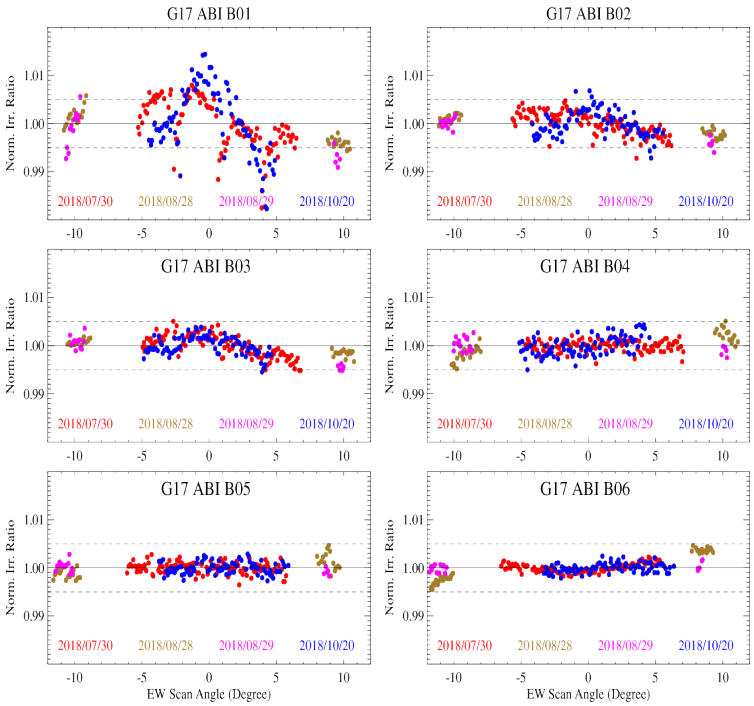

Figure 3. Same as Figure 2, but for G17.

It should be noted that the impact of the straylight on radiance calibration is negligible at the sample level. For B01, which is the most strongly affected by straylight, the impact is less than 0.01% on albedo for a typical Earth scene with a 40% albedo. However, even this small calibration error can accumulate in the calculated lunar irradiance with Equation 2, leading to variations of up to 1% in the irradiance ratio, as shown in Figures 2 and 3.

Based on the root causes and different instrument response performances at GOES-16 and 17, we apply different straylight correction methods to improve the calibration accuracy for B01-B03 images of the two ABIs.

Corrections of straylight in the B01-B03 spacelook scenes

The straylight, which is typically < 1-2 counts out of the 14-bit depth of the ABI calibration data, may appear in the spacelook scenes near the polar regions for both satellites. However, the operational conditions for GOES-16 and GOES-17 differ. Unlike GOES-16, which operates with a controlled focal plane module (FPM) temperature for the VNIR bands as originally designed, GOES-17 has a cryocooler anomaly and its VNIR FPM temperature is uncontrolled during operation [4]. As a result, GOES-17 data may experience variations in the FPM temperature during the chasing events. Two distinct methods were applied to correct the contaminated spacelook value. For events with stable FPM temperatures (<0.1 K drift), including all the GOES-16 events and one GOES-17 event, the mean spacelook counts near the Equator were used to represent the spacelook and re-calibrate the sample radiance within a timeline. For the GOES-17 events with more than 0.1 K temperature change, a linear regression between the FPM temperature and detector response was used to estimate the detector response at the spacelook times. The corrected spacelook was used to re-calibrate the radiance in B01-B03 lunar images.

Radiance correction for B01-B03 lunar images

After correcting for spacelook straylight, it was found that the normalized ratio increased when the Moon was close to the illuminated Earth at B01-B03. A similar pattern was also observed in a long space swath for GOES-17 when it was in a rolled position in its early in-orbit time before the PLT/PLPT started. This elevated irradiance was attributed to light spill from the illuminated Earth affecting the lunar images. The magnitude of this variation was similar to the impact of contaminated spacelook scenes. The average radiance from two 10×N samples (each located at the either edge of a lunar image) was used as an offset to correct the spilled radiance.

Here, N represents the number of valid detectors for each band.

doi: 10.25923/bm5d-xb98

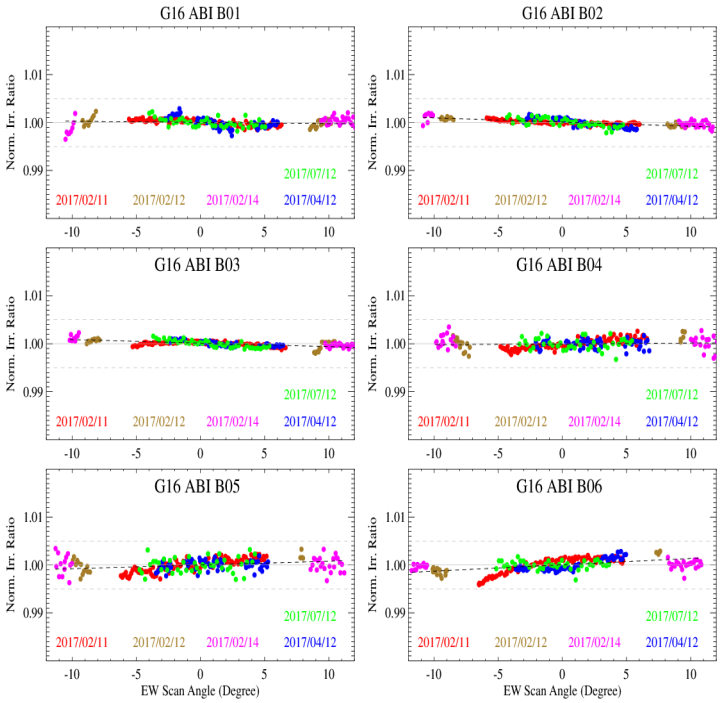

Figure 4. EW angle of incidence dependent lunar irradiance ratio for the six VNIR bands of G16. The B01-B03 images are calibrated with the corrected spacelook and image straylight correction. The B04-B06 data are same as shown in Figure 2.

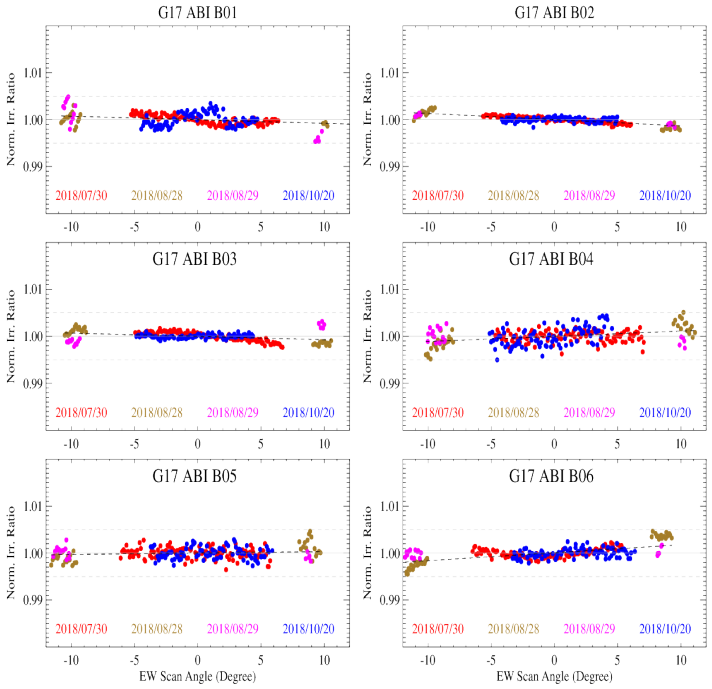

Figure 5: Same as Figure 4, but for G17.

This method assumes that the spilled light changes gradually across a subset lunar image and can therefore be represented with the mean value from the two ends. Using this newly derived sample radiance, we recalculated the lunar irradiance and the normalized lunar irradiance ratio for B01-B03 with Equations 1 and 2.

The final RVS results for B01-B03, after the straylight corrections, are shown in Figures 4 and 5 for GOES-16 and GOES-17, respectively, alongside for B04-B06. All the normalized irradiance ratios for all six VNIR bands on both satellites fall within 0.5% range. Furthermore, the RVS differences at the two ends of a full-disk ABI image, which ranges between -8.7° to + 8.7°, are less than 0.3% for all the VNIR bands. This study also confirms that the GIRO model has high relative accuracy for the ABI VNIR bands when the lunar images are collected within a relatively short time. The method outlined in this article can be applied to validate the EW spatial uniformity for imagers on other geostationary satellites, including the recently launched GOES-18 and the future GOES-U satellites.

Acknowledgements: The authors would like to thank NOAA GOES-R PRO, Flight and MOST teams for helping to collect the special scan data and EUMETSAT for sharing the GIRO model within the GSICS community. The scientific results and conclusion, as well as any reviews or opinions expressed herein, are those of the authors and do not necessarily reflect those of NOAA or Department of Commerce.

References

[1] Yu, F., X. Wu, X. Shao, and H. Qian, "Characterization of the East-West spatial uniformity for GOES-16/17 ABI bands using the Moon", *Remote Sensing*, 2023, 15, 1881. https://doi.org/10.3390/rs15071881.

[2] Yu, F., X. Wu, Stone, T., and G. Rindic-Ranic, "Angular variation of GOES Imager scan mirror visible reflectivity", *GSICS Quarterly,* 2013, 7(3), 9-10. https://repository.library.noaa.gov/view/noaa/17917.

[3] EUMETSAT. "GIRO and GSICS lunar observation dataset usage policy", 2015, http://gsics.atmos.umd.edu/pub/Development/LunarWorkArea/GSICS-EP-16_Doc_13_GIRO-GLOD-policy.pdf

[4]Van Naarden, J. and Lindsey, D., "Saving GOES-17", https://aerospaceamerica.aiaa.org/departments/saving-goes-17/ (2019)

doi: 10.25923/bm5d-xb98

A Lunar Eclipse Observation With AMSU-B

By Martin Burgdorf (Universität Hamburg), Niutao Liu (Fudan University), Stefan Buehler (Universität Hamburg), Ya-Qiu Jin (Fudan University) and Marc Prange (Universität Hamburg)

To establish the Moon as a flux reference for the calibration of microwave sounders, it is important to have both an accurate radiative transfer model and a precise measurement technique for the spaceborne instruments. A lot of effort was invested during the last few decades on improving lunar models, but often the achievable calibration precision was limited by uncertainties of the observations – both with microwave and optical instruments. To demonstrate that observations of the Moon with microwave sounders are at least as accurate as the ones performed with ground-based radio telescopes, we have analyzed observations of the Moon that were taken with AMSU-B (Advanced Microwave Sounding Unit - B) on NOAA-15 during the total lunar eclipse of 2004 October 28. The Moon appeared in its DSVs (Deep Space View) once per orbit of the spacecraft over the whole duration of the eclipse. In each of these orbits, the Moon produced an anomaly in the counts of the DSVs that lasted several minutes and had the shape of a Gaussian. From the counts obtained before and after the Moon intrusion, it was possible to calculate the gain and then the radiance of the Moon in each channel, i.e. at 89, 150, and 183 GHz. The processing steps are listed as IDL commands in [1].

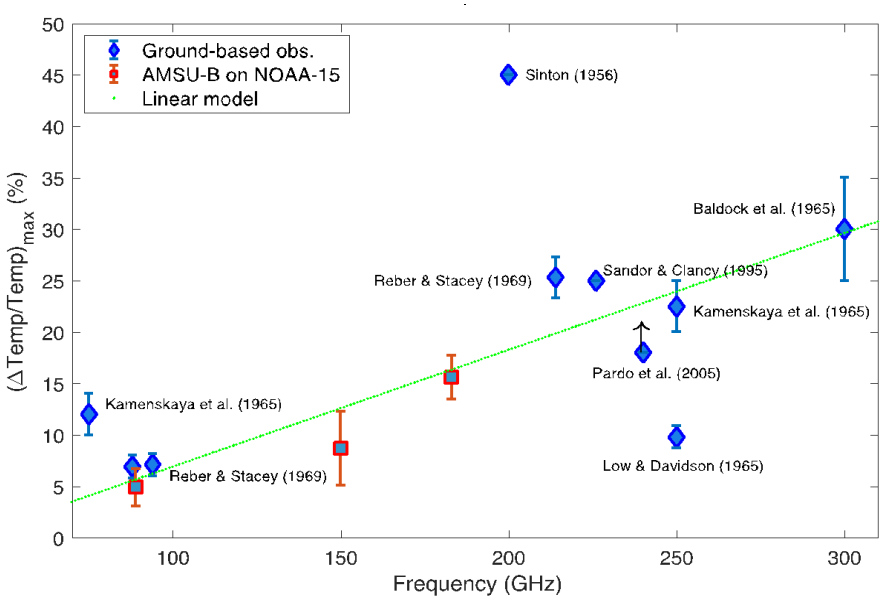

Figure 1. Maximum relative drop in effective temperature during different total lunar eclipses. Our results are shown as red rectangles.

Uncertainty of the Measured Brightness Temperature

The measurement of the relative drop in disk-integrated brightness temperature of the Moon during the eclipse has the advantage of being independent of the absolute flux calibration, which affects all observations in the same way. Another peculiarity of our observations of the Moon, however, introduces an additional uncertainty, and that is the distance of the Moon from the pointing direction of the deep space view. As the Moon fills only a fraction of the Gaussian beam, its signal decreases with increasing distance from the center of the beam. The Moon angle can be calculated with a program in the ATOVS and AVHRR pre-processing package, but the absolute pointing accuracy of the microwave sounders is only 0.2°, i.e., almost 20% of the FWHM of the beam. It is therefore necessary to determine the Moon angle in a more accurate way, and for this purpose we take advantage of the fact that there are four DSVs with slightly different pointing directions. The ratio of the maximum counts in the different DSVs is characteristic for the position of the Moon: In one orbit, two neighboring DSVs may produce very similar counts, indicating that the Moon is in the middle between them, and in the next orbit one DSV produces many more counts than its neighbors, indicating that the Moon is very close to this pointing direction. From comparing many observations of the full Moon without eclipse to a model, we found out how the measured counts depended on the position of the Moon relative to the four DSVs. From the random scatter of these counts we could determine the uncertainty of the measured brightness temperature: It is 5 K at 89 GHz for a single measurement with AMSU-B, when the Moon is in the center of a pointing direction, and somewhat larger, when the Moon falls in between two DSVs. For MHS (Microwave Humidity Sounder), the uncertainty is half as large.

By comparing the counts obtained from observations of the Moon during the eclipse to those without eclipse, but with the same Moon angle, we could calculate the maximum relative temperature drop at the different frequencies of AMSU-B. These values

are shown in the figure, and they demonstrate that the reliability of the observations with NOAA-15 allows to identify outliers in the results obtained with astronomical radio telescopes at similar frequencies [2].

Relevance to Detecting Calibration Trends

From comparing observations, where the Moon had different positions relative to the four DSVs, but the same phase angle, we could determine how the counts depend on the distance of the Moon from the pointing direction of the instrument. With this knowledge it is possible to calculate the brightness temperature from almost every appearance of the Moon in the DSV. There are about a hundred events like this per year, and the uncertainty of a single measurement is some 3K at 89 and 183 GHz for MHS. Hence one can detect a calibration trend of 0.1% between the first and last two years of the operational phase of a satellite. With a typical lifetime of ten years, this means that a trend of about 1%/decade in upper tropospheric humidity (for a typical UTH of 30%) can be detected, assuming that UTH is an exponential function of brightness temperature. This is smaller than the discrepancies between different moistening trends of UTH reported in the literature [3]. It will be interesting to check whether these results were affected by calibration trends.

Summary

We demonstrated how the radiance of the Moon during a total eclipse can be measured very precisely with AMSU-B, and we identified several wrong results obtained in the past with astronomical radio telescopes at similar wavelengths. The small uncertainties we achieved suggest that by analyzing all observations of the Moon that happened with microwave sounders in the past, it will be possible to check for undetected calibration drifts in the moistening trends of the upper tropospheric humidity.

References:

[1] IDL file available on request.

[2] Burgdorf, M., et al, 2023, Observation of a Lunar Eclipse at 89, 150, and 183 GHz, Planet. Sci. J., Vol. 4, 112, 10.3847/PSJ/acd76e.

[3] Shi, L., et al., 2022, Assessing the consistency of satellite-derived upper tropospheric humidity measurements, Atmos. Meas. Tech., Vol. 15, 6949–6963, 10.5194/amt-15-6949-2022.

NEWS IN THIS QUARTER

23rd GSICS Executive Panel Meeting (GSICS-EP-23) held from 29–30 June 2023 in Tokyo Japan

By Heikki Pohjola (WMO), Mitch Goldberg (CCNY for EUMETSAT, NOAA ret.), Bojan Bojkov (EUMETSAT)), Lawrence Flynn (NOAA), Manik Bali (UMD), Kamaljit Ray (IMD) and Fangfang Yu (UMD)

The 23rd Session of the Global Space-based Inter-Calibration System Executive Panel (GSICS-EP-23) was held in a hybrid mode during 29-30 June 2023 in Tokyo, Japan. The meeting was hosted by the Japan Meteorological Agency (JMA) and supported by the GSICS Coordination Center at NOAA and the World Meteorological Organization (WMO). Over 25 GSICS members participated in the meeting, representing CMA, ESA, EUMETSAT, ISRO, JAXA, JMA, MOES, NASA, NIST, NOAA, SITP ROSHYDROMET and WMO. This included EP members from GSICS member agencies, members of WMO secretariat, GSICS Coordination Center, and Chairs of GSICS Groups and Subgroups. The meeting began with a review of the proposed agenda by the Outgoing EP-Chair Dr. Mitch Goldberg, Incoming EP-Chair Dr. Bojan Bojkov, WMO Secretariat , Mr. Heikki Pohjola and GCC Director Dr. Larry Flynn and the meeting attendees. ISRO was represented by Dr. Rashmi Sharma (in person) and Dr. Pradeep Thapliyal (remote) and NOAA EP participation was monitored by Mary Ann Kutney after Mitch Goldberg stepped down.

Notable Changes in GSICS roles

EUMETSAT GSICS EP representative, Dr. Bojan Bojkov, was unanimously appointed as the new chair of EP. NASA confirmed Dr. Jack Xiong as their GSICS EP representative. Dr. Mounir Lekouara (EUMETSAT) was nominated to be the incoming vice chair of the GRWG, and Mr. Paolo Castracane (ESA) was nominated to be the incoming vice chair of the GDWG.

doi: 10.25923/bm5d-xb98

GSICS EP Discussions

GSICS Coordination Center

The GSICS Coordination Center (GCC) Director, Dr. Larry Flynn, reported activities for the previous year and goals for the coming year. He thanked members for participation in the GSICS Annual Meeting in March 2023 hosted by NOAA in College Park, MD, USA. He mentioned that the interest in GSICS continues to be strong with almost 445 members registered for the messaging service. He highlighted that over 70 scientists contributed to articles in the GSICS Newsletter as the newsletter continues to be received very well by the community and beyond. Larry also briefed on new actions that GCC picked up earlier this year in the annual meeting 2023. He also mentioned that the four new GSICS Products produced by JMA (near-real-time and re-analysis for Himawari-9 vs. IASI-B & AIRS) were accepted following the GPPA family of instruments rule.

In the following discussion, the EP suggested two actions on GCC. All meeting actions can be found in the Action Tracker at https://www.star.nesdis.noaa.gov/smcd/GCC/MeetingActions.php.

GSICS Research Working Group

GSICS Research Working Group (GRWG) Chair, Fangfang Yu, presented a summary of GRWG activities over the past year. She reported that the 2023 GRWG annual (hybrid) meeting was successfully held 27 Feb to 3 March in 2023 in College Park, with strong support from EP, GCC, GDWG, and GRWG members. More than 65 people from international space and operational agencies, research institutes, universities, and private sectors attended the meetings. She reported progress made by each subgroup of GSICS Research Working Group.

- Infrared (IR) Subgroup: This subgroup focused on enhancing the inter-calibration algorithm for GEO-LEO IR instruments, explored GEO-GEO inter-comparison applications, and investigated the possibility of inter-calibrating instruments on Low Earth Orbit (LEO) satellites.
- Microwave (MW) Subgroup: The MW subgroup engaged in technical discussions concerning inter-calibration methods for microwave instruments and the calibration/validation activities of both existing and upcoming MW instruments. They reached an agreement to establish an uncertainty framework for comparing instrument measurements.
- Visible and Near-Infrared (VIS/NIR) Subgroup: This subgroup conducted six monthly web-meetings that primarily revolved around visible imager and visible calibration strategies. Additionally, they are actively working on implementing a new GSICS lunar model for calibration purposes.
- UV/VIS/NIR Spectrometers (UVN-S) Subgroup: The UVN-S subgroup provided Calibration and Validation (Cal/Val) updates on various instruments, including those that are in the past, End-of-Life, "operational," newer, and upcoming launch categories. They discussed studies related to solar irradiance and product comparisons. Furthermore, they recommended continued participation in the OCO-TROPOMI-GOSAT calibration team meeting and

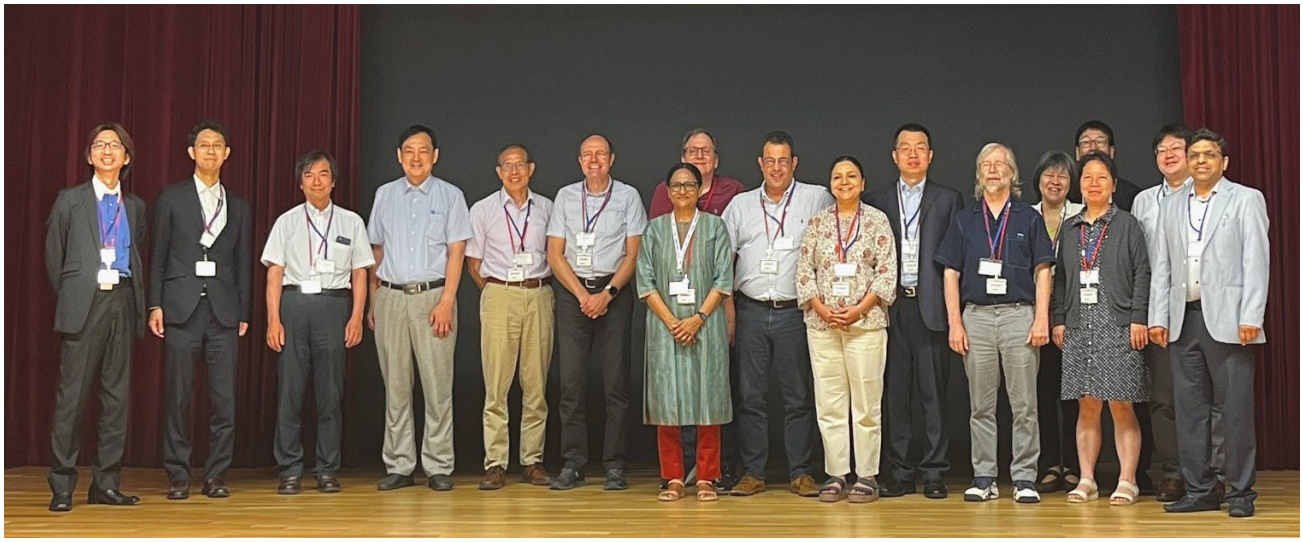

Photo: Participants in the GSICS EP-23, JMA Tokyo, Japan

doi: 10.25923/bm5d-xb98

the hosting of monthly subgroup meetings to focus on comparison and calibration activities related to UV/VIS/NIR spectrometers.

GSICS Data Working Group

GSICs Data Working group (GDWG) Chair , Dr. Kamaljit Ray presented the GDWG report and summarized several key activities by GSICS member agencies and presented the GDWG work plan. Some of the topics that GDWG Chair covered included the new Membership, ESA's EVDC website, PI-MED website and salinity website, that aim to help the calibration community with access to state-of-the-art calibration data. The Data working group also reported the reprocessing activity at CMA, where they deployed the GSICS corrections on a massive database, dating back decades and reprocessed the entire Earth Observation data record obtained from Chinese Satellites. EP proceeded to give the following recommendation to the GSICS members.

Space Weather Subgroup

The GSICS EP endorsed and accepted GSICS Space Weather (GSW) as a new subgroup under the GRWG umbrella with Dr. Tsutomu Nagatsuma from NICT as the GSW subgroup chair. Nagatsuma San stated that, earlier this year for the first time GSW organized a breakout session in the annual meeting. He also reported that, in the coming year, its initial focus will be on high-energy particle sensors on GEO. It will propose applications produced from multiple satellite data and methods of near-real time and archival inter-calibration, harmonizing data levels and finally define GSICS products and tools for space weather sensors.

Pre-Flight calibration workshop

At the executive Panel meeting, Philippe Goryl presented the plan for the joint CEOS-WGCV CGMS-GSICS Pre-Flight calibration workshop to be organized in November 2024 at ESA ESTEC in the Netherlands.

Users' feedback

The International Satellite Cloud Climatology Project (ISCCP) and GSICS share a user producer relationship. Larry Flynn shared the feedback of the (ISCCP) on using GSICS products.

Future GSICS Meetings

Finally, the EP concluded with discussion on future GSICS Annual Meeting and the GSICS EP meeting.

It was decided that the next Annual Meeting would be hosted by EUMETSAT in March 2024 and held immediately before the GSICS EP meeting.

Final Actions, Decisions, and Recommendation, including detailed contributions from each GSICS member agency are currently being finalized and will be posted at the https://community.wmo.int/en/meetings/gsics-ep-23 .

Summary of the CEOS WGCV-52 Meeting

By Philippe Goryl (ESA) and Paolo Castracane (Rhea System for ESA)

Meeting Summary

The 52nd Meeting of the Working Group on Calibration and Validation (WGCV-52) was held in ESA/ESRIN, Frascati, Italy June 5th-9th, 2023. The workshop started with ESA presentations focused on current and future EO Missions, Cal/Val and data quality activities. A session was dedicated on the future ESA/JAXA Mission EarthCARE (launch planned for 2024), it includes active sensors for detecting clouds and aerosols, as well as passive sensors capable of measuring the returning radiation. The ESA-JAXA Pre-Launch Earth CARE Science and Validation Workshop is scheduled for 13-17 November 2023, ESA-ESRIN Frascati, Italy.

The CEOS Work Plan and Actions were reviewed: SI-Traceable Satellite (SITSat) topics were discussed including the motivation for having a SITSat task team that may include representatives from GSICS.

WGCV contributions to the CEOS New Space Task Team (NSTT) were discussed; WGCV in coordination with GSICS provides inputs to the NSTT in terms of Cal/Val references, methods, protocols, tools and expertise. It was highlighted that the WGCV is also involved with New Space through JACIE and VH-RODA workshops. Two topics clearly emerged: the need of additional guidance for data quality assessment in the New Space context (the Maturity Matrix approach was suggested) and the idea to create a so-called radiometric matchup database by acquiring a series of data over specific sites and making it available through an open system for sharing and comparison. The discussion for having Ground Control Points (GCPs) database for Very High-Resolution Sensors also generated a clear interest and triggered a corresponding action to bring this topic for the Terrain Mapping Subgroup meeting.

doi: 10.25923/bm5d-xb98

Since the hyperspectral domain has been recognized as an emerging priority, a session was dedicated to this topic. The last updates on Hypernets were presented and a guidance CEOS document entitled "Hyperspectral Cal/Val resources" was shown with the aim to get further feedback from the WGCV community.

Following the example of RadCalNET, WGCV is now supporting the establishment of a coordinated network for SAR Cal/Val (SARCalNet) and a network dedicated to Thermal Infrared Cal/Val (TIRCalNet) that will be relevant for LSTM, SBG or TRISHNA missions, but also for New Space Thermal Infrared missions.

In the atmospheric domain, the Boundary-layer Air Quality-analysis Using Network of Instrument (BAQUNIN) supersite activities were presented. The BAQUNIN Super-Site includes ground based active and passive remote sensing instruments operating in synergy, offering quantitative and qualitative information for a wide range of atmospheric parameters for atmospheric chemistry (satellite) validation activities and Planetary Boundary Layer (PBL) studies. The need to find a mechanism to support GHG networks for Cal/Val activities has been also emphasized (action raised up to CEOS leadership level) In particular, the use and support to NDACC, TCCON, COCCON were discussed.

WGCV reviewed the CEOS Fiducial Reference Measurement (FRM) assessment framework process; the document intends to provide a roadmap toward an assessment structure based on a Maturity Matrix approach (EDAP-like) and including categories on: Nature of FRM, instrumentation, Operation/Sampling, Data, Metrology and a Verification process from and independent assessor. It serves as a tool to communicate and interact with data providers and to motivate them. The FRM concept was developed specifically for satellite calibration and validation, distinguishing it from in situ measurements.

Finally, the latest updates on the CEOS WGCV CalVal portal were presented. A session was dedicated to the WGCV and GSICS Collaborations including the report on GSCIS 2023 Annual meeting held in College Park, USA. It was highlighted as WGCV and GSICS share methods and protocols, and both look for references. Common topics were indicated including the following: SITSats, FRM assessment framework, and New Space.

In particular, plans for "CEOS/GSICS pre-flight calibration and characterisation" workshop were discussed. The workshop will take place at ESA/ESTEC in the Netherlands on 19-21 November 2024.

The WGCV-52 Workshop has been concluded with the plan for next WGCV-53 Meeting; CONAE offered to host the meeting in Argentina, Cordoba in March 2024.

Photo: Participants of the WGCV-52 meeting at ESA/ESRIN, Frascati, Italy

doi: 10.25923/bm5d-xb98

Tropospheric Emissions: Monitoring of Pollution (TEMPO) sends first light images of NO_2 concentrations

By Manik Bali (UMD) and Larry Flynn NOAA)

On Aug 24, 2023, NASA released the first light images from the Tropospheric Emissions: Monitoring of Pollution (TEMPO) mission [1]. The images showed NO_2 concentrations over the continental United States.

TEMPO is situated in a geostationary orbit at 91º West. From its geostationary position TEMPO can take diurnal measurements of atmospheric composition. It is the first space-based instrument designed to continuously measure air quality above North America with the resolution of a tens of km^2.

TEMPO is a key component of the GEO-AQ Air Quality constellation [2] and joins two other similar instruments, the GEMS (128º E) and the Sentinel-4 (0º E to be launch in 2024) that make measurements in UV VIS/NIR spectral ranges and are designed to monitor atmospheric pollutants and trace gasses.

From a GSICS standpoint, this instrument is also helpful as it gives inter-calibration opportunities with under flights of LEO instruments.

References:

1. NASA Press Release Aug 2023: NASA Shares First Images from US Pollution-Monitoring Instrument

2. CEOS Atmospheric Composition Virtual Constellation and the CEOS Working Group on Calibration and Validation Version 1.1, 2nd October 2019 Geostationary Satellite Constellation for Observing Global Air Quality: GeoPhysical Validation Needs.

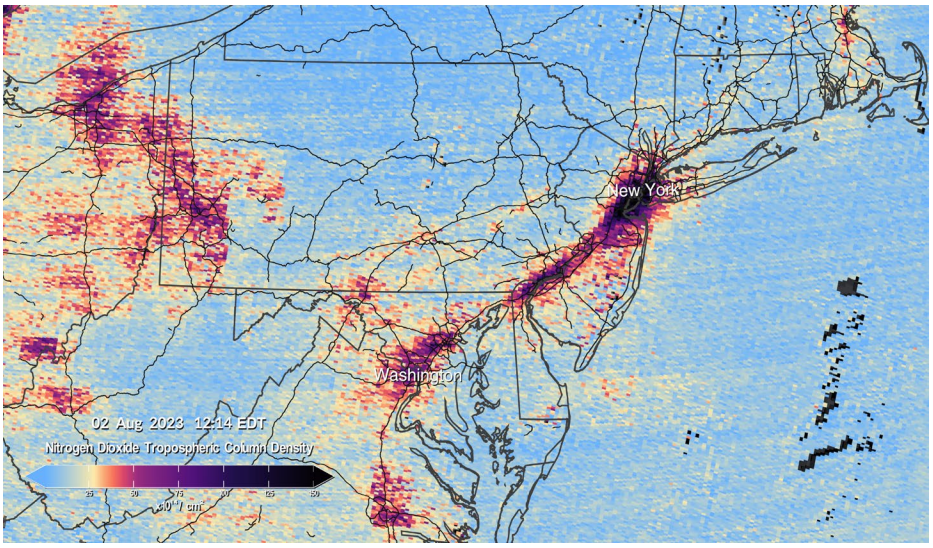

Image Above: First light image shows nitrogen dioxide levels over the DC/Philadelphia/New York region at 12:14 on August 2, 2023, as measured by TEMPO [1]. *Credits:* Kel Elkins, Trent Schindler, and Cindy Starr/NASA's Scientific Visualization Studio

	GEMS	Sentinel-4	TEMPO
Orbit	Geostationary	Geostationary	Geostationary
Domain	Asia-Pacific	Europe and surrounding	North America
Revisit	1 hour	1 hour	1 hour
Host satellite	GEO-KOMPSAT-2B	MTG-S	Intelsat 40e
Launch	February 2020	2024	April 2023
Spectral	UV-Vis 300-500 nm	UV-Vis 305-500, NIR 750-775 nm	UV-Vis 293-490, Vis 540-740 nm
Key Products	O_3, NO_2, SO_2, HCHO, CHOCHO, aerosol	O_3, NO_2, SO_2, HCHO, CHOCHO, aerosol	O_3, NO_2, SO_2, HCHO, CHOCHO, aerosol
Spatial	3.5 km N/S × 8 km E/W @38N	8 km × 8 km @45N	2.1 km N/S × 4.7 km E/W @35N
Product resolution	7 km N/S × 8 km E/W @38N (gas), 3.5 km N/S × 8 km E/W @38N (aerosol)	8.9 km N/S × 11.7 km E/W @45N	8.4 km N/S × 4.7 km E/W or better @35N
Notes	Synergy with AMI and GOCI-2 instruments w.r.t. aerosol and clouds.	Two instruments in sequence. Synergy with IR sounder on MTG-S w.r.t. ozone. Synergy with FCI imager on MTG-I w.r.t. aerosol and clouds.	GEO-ACX precursor. Synergy with GOES-R/S ABI w.r.t. aerosol and clouds.

Table Above: Comparison of TEMPO, GEMS and Sentinel-4 [2]

ANNOUNCEMENTS

AOMSUC-13 to be held as an in-person event 03-10 November 2023

By Allen Huang, SSEC, University of Wisconsin-Madison

The 13th Asia-Oceania Meteorological Satellite Users' Conference (AOMSUC-13) will be held virtually on 03-10 November 2023. Details can be found on the conference web page, including the first announcement and the registration information: https://nmsc.kma.go.kr/enhome/html/conference/AOMSUC_2023.do

The sessions of the AOMSUC conferences are:

1. The space program and data access updates
2. SmallSat/Cubesat for meteorology, climate, and environmental monitoring
3. Application for numerical weather prediction
4. Application for weather analysis and nowcasting
5. Application for land surface and sea surface derived from satellite observations
6. Space weather
7. Performance and calibration of satellite instruments

AOMSUC-13 is planning to hold three events:

- Comprehensive training event on satellite data and product utilization in Jincheon.
- The AOMSUC-13 plenary and scientific sessions in Busan.
- Joint RA-II and RA-V coordination meeting(by invitation) in Busan.

The deadline for submission is Deadline for abstract submission is 18 September 2023.

GSICS-Related Publications

Heyu Xu, Wenxin Huang, Xiaolong Si, Qingjun Song, Xin Li, Xu Weiwei, Yue Ma, and Liming Zhang, "Radiometric cross-calibration of Sentinel-2B MSI with HY-1C SCS based on the near simultaneous imaging of common ground targets," Opt. Express 31, 3619-3637 (2023) https://doi.org/10.1364/OE.479445

Lee Jae-Deok, Kim Se-Young, Lee Jong-Hwan, Yi Dong-Woo, Ryu Ji-Ho, Sung Jin-Bong, "Calibration Path Pattern Synthesis Technique for Satellite SAR Payload", J. Korean Inst. Electromagn. Eng. Sci. 2023;34(3):232-235. https://doi.org/10.5515/KJKIEES.2023.34.3.232

Yu, F.; Wu, X.; Shao, X.; Qian, H. Characterization of the East—West Spatial Uniformity for GOES-16/17 ABI Bands Using the Moon. *Remote Sens.* **2023**, *15*, 1881. https://doi.org/10.3390/rs15071881

Naethe, P., Asgari, M., Kneer, C. *et al.* Calibration and Validation from Ground to Airborne and Satellite Level: Joint Application of Time-Synchronous Field Spectroscopy, Drone, Aircraft and Sentinel-2 Imaging. *PFG* **91**, 43–58 (2023). https://doi.org/10.1007/s41064-022-00231-x

S. J. Smith *et al*., "Correcting Gain Drift in TES Detectors for Future X-Ray Satellite Missions," in *IEEE Transactions on Applied Superconductivity*, vol. 33, no. 5, pp. 1-6, Aug. 2023, Art no. 2101006, doi: https://doi.org/10/1007/10.1109/TASC.2023.3258908

Tang, H.; Xie, J.; Chen, W.; Zhang, H.; Wang, H., Absolute Radiometric Calibration of ZY3-02 Satellite Multispectral Imager Based on Irradiance-Based Method. *Remote Sens.* **2023**, *15*, 448. https://doi.org/10.3390/rs15020448

Withanage, D.C.; Teramoto, M.; Cho, M., On-Orbit Magnetometer Data Calibration Using Genetic Algorithm and Interchangeability of the Calibration Parameters. *Appl. Sci.* **2023**, *13*, 6742. https://doi.org/10.3390/app13116742

Submitting Articles to the GSICS Quarterly Newsletter:

The GSICS Quarterly Press Crew is looking for short articles (800 to 900 words with one or two key, simple illustrations), especially related to calibration / validation capabilities and how they have been used to positively impact weather and climate products. Unsolicited articles may be submitted for consideration anytime, and if accepted, will be published in the next available newsletter issue after approval / editing. Please send articles to manik.bali@noaa.gov . Preference will be given to articles summarizing published results on instrument calibration.

With Help from our friends:

The GSICS Quarterly Editor would like to thank, Cheng-Zi Zou (NOAA), Sri Harsha Madhavan (NASA), and Lawrence E. Flynn (NOAA) for reviewing articles in this issue. Special thanks to Jan Thomas (NOAA) in helping with 508 compliance and submission process.

Published By

GSICS Coordination Center
NOAA/NESDIS/STAR
National Center for Weather & Climate Prediction,
5830 University Research Court
College Park, MD 20740, USA